Supporting Information

- 1 -

A hampered oxidative addition of pre-coordinated pincer ligands can favour alternative pathways of activation

Frerk-Ulfert Wehmeyer[a] and Robert Langer[a,*]

[a] *Institute of Chemistry, Faculty of Natural Sciences II, Martin-Luther-Universität Halle- Wittenberg, Kurt-Mothes-Str. 2, D-06120 Halle (Saale), Germany. Fax: +49 (0)345 5527028; Tel: +49 (0)345 5525620; E-mail:* robert.langer@chemie.uni-halle.de

Contents

1. Experimental Procedures

1.1 Materials and Methods

All experiments were carried out under an atmosphere of purified argon 5.0 in the MBraun LABmaster and GS MEGA glove box or using standard Schlenk techniques.

Diethylether, tetrahydrofuran and toluene were dried over Na. *n*-Hexane was dried over $LiAlH_4$. Dichloromethane and MeCN were dried over CaH_2. After drying, solvents were stored over appropriate molecular sieves. Deuterated solvents were degassed with freeze-pump-thaw cycles and stored over appropriate molecular sieves under argon atmosphere.

^1H, ^{13}C, ^{11}B, ^{19}F and ^{31}P NMR spectra were recorded using Agilent Technologies 400 MHz VNMRS and 500 MHz DD2 NMR spectrometers at 300 K. ^1H and ^{13}C {^1H}, ^{13}C-APT (attached proton test) NMR chemical shifts are reported in ppm referenced to tetramethylsilane. The resonance of the residual protons in the deuterated solvent was used as internal reference for ^1H NMR spectra. The solvent peak of the deuterated solvent was used as internal reference for ^{13}C NMR spectra. ^{11}B NMR chemical shifts are reported in ppm referenced to $BF_3(OEt_2)$ as external standard. ^{19}F NMR chemical shifts are reported in ppm with respect to $CFCl_3$ and referenced to liquid $CFCl_3$ as external standard. ^{31}P NMR chemical shifts are reported in ppm with respect to H_3PO_4 and referenced to an external 85 % solution of phosphoric acid in D_2O. The following abbreviations are used for the description of NMR data: br (broad), s (singlet), d (doublet), t (triplet), q (quartet), quin (quintet), m (multiplet).

FT-IR spectra were recorded by attenuated total reflection (ATR) of the solid samples on a Bruker Tensor 27 spectrometer at ambient temperature. The intensity of the absorption band is indicated as w (weak), m (medium), s (strong), vs (very strong) and br (broad).

High-resolution mass spectra were recorded on a Thermo Scientific Q Exactive Plus spectrometer equipped with an Orbitrap Mass Analyzer and Thermo Scientific HESI-II (heated electro spray ionization). External mass calibration was performed in HESI mode by measuring calmix provided from Thermo Scientific. LTQ Velos ESI Positiv Ion Calibration Solution and ESI Negativ Ion Calibration Solution, respectively.

Elemental analyses by combustion analysis were performed in a Unicube (Elementar) using argon as carrier/shielding gas and tin foil crucibles for sample preparation, as well as in an Elementar-Vario EL using helium as carrier/shielding gas.

Bis(diphenylphosphino)methane (dppm) was synthesized following the procedure published by K. Sommer.[1] [H$_2$B(dppm)$_2$]Br (**1-Br**) was synthesized according to the previously reported procedure.[2]

1.2 Synthesis of [H$_2$B(dppm)$_2$](PF$_6$) (**1-PF$_6$**)

dppm (2000 mg, 5.2 mmol) and KPF$_6$ (479 mg, 2.6 mmol) were dissolved in 15 mL CH$_2$Cl$_2$ and a solution of BH$_2$Br·SMe$_2$ in CH$_2$Cl$_2$ (1 M, 2.6 mL, 2.6 mmol) was added. The solution was stirred for 15 days until no further conversion of dppm was observed in the ^{31}P{^{1}H} NMR spectral monitoring. The solution was layered with *n*-hexane, which resulted in a precipitation of **1-PF$_6$** after three days. The supernatant solution was decanted off and the precipitate was washed with Et$_2$O and dried *in vacuo*. Yield: 1560 mg (1.68 mmol, 64.6 %). Anal. Calcd for C$_{50}$H$_{46}$BF$_6$P$_5$: C, 64.81; H, 5.00. Found: C, 64.19; H, 4.65. ^{1}H NMR (499.72 MHz, CD$_2$Cl$_2$, 27 °C) δ = 2.53 (d, 4H, $^3J_{HH}$= 12.3 Hz, C*H$_2$*), 7.07 (m, 8H, phenyl-*H*), 7.18 (m, 8H, phenyl-*H*), 7.21-7.28 (m, 12H, phenyl-*H*), 7.34 (m, 8H, phenyl-*H*), 7.40 (m, 4H, phenyl-*H*) ppm. Only resonances that are changing upon ^{11}B decoupling are listed for the ^{1}H{^{11}B} NMR spectrum. ^{1}H{^{11}B} NMR (499.72 MHz, CD$_2$Cl$_2$, 27 °C) δ = 2.74 (t, 2H, $^2J_{PP}$ = 20.2 Hz) ppm. In the ^{1}H{^{31}P} NMR spectrum the resonance at 2.54 ppm is reduced to a singlet. ^{11}B{^{1}H} NMR (160.33 MHz, CD$_2$Cl$_2$, 27 °C) δ = -33.9 (br) ppm. ^{31}P{^{1}H} NMR (202.28 MHz, CD$_2$Cl$_2$, 27 °C) δ = -144.4 (sept, J_{PF} = 710.8 Hz, *P*-F), -30.3 (d, J_{PP} = 68.4 Hz), 6.6 (br, *P*-B-*P*) ppm. ^{19}F{^{1}H} NMR (470.16 MHz, CD$_2$Cl$_2$, 27 °C) δ = -73.2 (d, $^1J_{FP}$ = 710.7 Hz) ppm. ^{13}C APT NMR (125.67 MHz, CD$_2$Cl$_2$, 27 °C) δ = 22.9 (m, P-*C*H$_2$-P), 124.0 (m, phenyl-*C*), 124.5 (m, phenyl-*C*), 129.1 (d, J_{CP} = 8.0 Hz, phenyl-*C*), 129.9 (t, J_{CP} = 11.2 Hz, phenyl-*C*), 132.8 (s, phenyl-*C*), 132.9 (s, phenyl-*C*), 133.0 (phenyl-*C*),133.5 (d, J_{CP} = 2.8 Hz, phenyl-*C*), 136.3 (dd, J = 13.3 Hz, J = 7.3 Hz, phenyl-*C*) ppm. FT-IR (ATR) $\tilde{v}$ / cm^{-1}: 3055 (w), 3015 (w), 3003 (w), 2964 (w), 2908 (w), 2684 (w, b), 2453 (w), 2405 (w), 1886 (w), 1808 (w), 1586 (w), 1574 (w), 1483 (w), 1435 (m), 1331 (w), 1308 (w), 1276 (w), 1188 (w), 1161 (w), 1140 (w), 1108 (m), 1071 (w), 1028 (w), 999 (m), 984 (w), 919 (w), 873 (w), 833 (s), 818 (s), 777 (m), 739 (m), 733 (m), 722 (m), 688 (s), 634 (m), 590 (w), 556 (s), 510 (m), 495 (m), 464 (m), 447 (w), 399 (w), 383 (m), 340 (w), 267 (w), 249 (w), 225 (w), 204 (w).

1.3 Synthesis of [(HB{dppm}$_2$)PtCl](PF$_6$) (**2**)

[H$_2$B(dppm)$_2$](PF$_6$) (**1-PF$_6$**, 57.5 mg, 0.062 mmol) and PtCl$_2$ (15.0 mg, 0.056 mmol) were dissolved in 1 mL CH$_2$Cl$_2$ and the resulting solution was stirred for 30 min at ambient temperature. The solution was subsequently filtered via syringe filter (glass fibre 0.7 μm) and the purity was assessed by ^{31}P{^{1}H} NMR spectroscopy. The pure product was obtained by precipitating **2** from the CH$_2$Cl$_2$ solution and addition of 5 mL toluene, after repeated washing of the obtained solid with diethyl ether. Continuous drying of the resulting solid *in vacuo* yields 59.1 mg (0.051 mmol, 90.6 %) of **2**. Anal. Calcd for C$_{50}$H$_{45}$BClF$_6$P$_5$Pt: C, 51.95; H, 3.92. Found: C, 52.13; H, 3.78. ^{1}H NMR (499.72 MHz, CD$_2$Cl$_2$, 27 °C) δ = 3.70 (m, 4H, C*H$_2$*), 7.12 (m, 4H, phenyl-*H*), 7.25 (m, 8H, phenyl-*H*), 7.33 (m, 4H, phenyl-*H*), 7.42 (m, 12H, phenyl-*H*), 7.48 (m, 4H, phenyl-*H*), 7.74 (q, 4H, J_{HH} = 6.4 Hz, phenyl-*H*), 7.88 (q, 4H, J = 6.4 Hz, phenyl-*H*). Only resonances that are changing upon ^{11}B decoupling are listed for the ^{1}H{^{11}B} NMR spectrum. ^{1}H{^{11}B} NMR (499.72 MHz, CD$_2$Cl$_2$, 27 °C) δ = 3.86 (m, 1H, B*H*) ppm. In the ^{1}H{^{31}P} NMR spectrum the multiplicity of the signals at 3.70, 7.12, 7.42, 7.48, 7.74 and 7.88 Hz is reduced. ^{31}P{^{1}H} NMR (202.28 MHz, CD$_2$Cl$_2$, 27 °C) δ = -144.4 (sept, $^1J_{PF}$ = 711.1 Hz, *P*F$_6$), 17.5 (br, *P*-B-*P*), 21.6 (m, *P*-Pt-*P*, with ^{195}Pt-satellites $^1J_{PPt}$ = 2988,5 Hz) ppm. ^{19}F{^{1}H} NMR (470.16 MHz, CD$_2$Cl$_2$, 27 °C) δ = -72.9 (d, $^1J_{FP}$ = 711.1 Hz) ppm. ^{13}C APT NMR (125.67 MHz, CD$_2$Cl$_2$, 27 °C) δ = 34.7 (m, P-*C*H$_2$-P), 122.6 (t, J = 31.3 Hz, phenyl-*C*), 124.2 (t, J = 30.1 Hz, phenyl-*C*), 129.4 (t, J = 5.6 Hz, phenyl-*C*), 129.5 (t, J = 5.6 Hz, phenyl-*C*), 129.9 (t, J = 5.5 Hz, phenyl-*C*), 130.0 (t, J = 5.4 Hz, phenyl-*C*), 130.4 (t, J = 28.3 Hz, phenyl-*C*), 132.0 (s, phenyl-*C*), 132.7 (t, J = 5.0 Hz, phenyl-*C*), 133.2 (t, J = 4.9 Hz, phenyl-*C*), 133.4 (s, phenyl-*C*), 133.6 (s, phenyl-*C*), 133.9 (t, J = 7.1 Hz, phenyl-*C*), 134.4 (t, J = 6.9 Hz, phenyl-*C* ppm. ^{11}B{^{1}H} NMR (160.33 MHz, CD$_2$Cl$_2$, 27 °C) δ = -27.2 (br t, $^1J_{BP}$ = 282.9 Hz, P-*B*) ppm. FT-IR (ATR) û / cm^{-1}: 3055 (w), 2916 (w), 2684 (w), 2333 (w), 1963 (w), 1894 (w), 1812 (w), 1587 (w), 1574 (w), 1483 (w), 1435 (m), 1390 (w), 1365 (w), 1335 (w), 1310 (w), 1279 (w), 1189 (w), 1161 (w), 1132 (w), 1100 (m), 1027 (w), 999 (w), 924 (w), 831 (s), 789 (m), 774 (m), 736 (s), 686 (s), 616 (w), 555 (s), 520 (s), 482 (s), 466 (s), 394 (m), 368 (m), 327 (m), 261 (m), 224 (m), 211 (w). HR-HESI-MS (pos. mode) m/z: 1010.19059 (calculated for [(HB{dppm}$_2$)PtCl]$^+$), 1011.19061 (found, Δ = 0.02 ppm).

1.4 Synthesis of [(dppm)(H$_2$B{dppm})Pt]Br (**3**)

Pt(PPh$_3$)$_4$ (100.0 mg, 0.084 mmol) and [H$_2$B(dppm)$_2$]Br (**1-Br**, 69.2 mg 0.084 mmol) were dissolved in 1 mL THF and the resulting solution was stirred for 30 min at ambient temperature. After a short period of time a white solid started to precipitate. After 1 h the solid was collected on a syringe filter and subsequently removed from the filter by addition of 1 mL CH$_2$Cl$_2$. The pure product was obtained by precipitating **3** from the CH$_2$Cl$_2$ solution and addition of 5 mL toluene. The supernatant solution was decanted and the obtained solid was repeatedly washed with diethyl ether.

Continuous drying of the resulting solid *in vacuo* yields 30.0 mg (0.0035 mmol, 35.3 %) of **3**. Complex **3** can be formed with **1-PF$_6$** instead of **1-Br** as well, likely due to the presence of fluoride ions, formed by hydrolysis of the PF$_6$ counter ion. Crystallisation with a PF$_6$-counter ion gives rise to single crystals of suitable quality for scXRD analysis. Anal. Calcd for C$_{50}$H$_{46}$BF$_6$P$_5$Pt·0.7C$_7$H$_8$: C, 55.59; H, 4.39. Found: C, 55.69; H, 4.35. ^{1}H NMR (499.72 MHz, CD$_2$Cl$_2$, 27 °C) δ = 2.61 (br, 2H, BH_2), 3.62 (m, 2H, CH_2), 4.78 (m, 2H, CH_2), 7.03 (m, 4H, phenyl-H), 7.18 (m, 8H, phenyl-H), 7.26 (td, 4H, J_{HH} = 8.0 Hz, J_{HH} = 2.3 Hz, phenyl-H), 7.34 (m, 8H, phenyl-H), 7.44 (m, 2H, phenyl-H), 7.49-7.61 (m, 10H, phenyl-H), 7.77 (m, 4H, phenyl-H) ppm. Only resonances that are changing upon decoupling are listed for the ^{1}H{^{11}B} NMR spectrum. ^{1}H{^{11}B} NMR (499.72 MHz, CD$_2$Cl$_2$, 27 °C) δ = 2.61 (br t, 1H, $^2J_{HP}$ = 27.6 Hz, BH) ppm. In the ^{1}H{^{31}P} NMR spectrum the multiplicity of the signals at 3.62, 4.78, 7.03, 7.18, 7.26, 7.44, 7.49-7.61, 7.77 ppm is reduced. ^{31}P{^{1}H} NMR (202.28 MHz, CD$_2$Cl$_2$, 27 °C) δ = -17.2 (dm, J_{PP} = 378.0 Hz, with ^{195}Pt-satellites $^1J_{PPt}$ = 2872.0 Hz), -15.5 (br, with ^{195}Pt-satellites J_{PPt} = 884.7 Hz), 28.5-30.7 (br), 32.7 (ddd, J_{PP} = 377.0 Hz, J_{PP} = 117.8 Hz, J_{PP} = 23.6 Hz, with ^{195}Pt-satellites $^1J_{PPt}$ = 3095.7 Hz) ppm. ^{13}C APT NMR (125.67 MHz, CD$_2$Cl$_2$, 27 °C) δ = 129.5 (t, J = 10.6 Hz, phenyl-C), 129.6 (dd, J = 21.0 Hz, 10.6 Hz, phenyl-C), 131.8 (dd, J = 43.86 Hz, 2.16 Hz, phenyl-C), 132.3 (dd, J = 12.1 Hz, 2.37 Hz, phenyl-C), 132.9 (s, phenyl-C), 133.0 (s, phenyl-C), 133.1 (s, phenyl-C), 133.4 (d, J = 12.1 Hz, phenyl-C), 133.8 (d, J = 12.6 Hz, phenyl-C) ppm. ^{11}B{^{1}H} NMR (160.33 MHz, CD$_2$Cl$_2$, 27 °C) δ = -29.9 (br) ppm. FT-IR (ATR) û / cm^{-1}: 3048 (w), 2924 (w), 2856 (w), 2379 (w), 2342 (w), 1481 (w), 1434 (m), 1368 (w), 1308 (w), 1275 (w), 1186 (w), 1159 (w), 1136 (w), 1102 (m), 1069 (w), 1027 (w), 997 (w), 894 (w), 847 (w), 823 (w), 791 (m), 740 (s), 727 (s), 710 (m), 690 (s), 638 (w), 617 (w), 573 (w), 541 (w), 526 (m), 498 (s), 486 (m), 476 (m), 457 (m), 443 (m), 433 (m), 362 (m), 342 (m), 289 (w), 261 (w), 229 (w), 218 (w), 203 (w). HR-HESI-MS (pos. mode) m/z: 976.22966 (calculated for [(dppm)(H$_2$B{dppm})Pt]$^+$), 976.22931 (found, Δ = 0.35 ppm).

2. Details for *cis*- and *trans*-influence

As $^1J_{PtP}$-coupling constants can be used as an estimate of the Pt–P-bond strength,[3] we analysed different Pt^{II} chlorido pincer complexes, containing a pincer-type ligand with terminal PPh$_2$ groups (Table 1), to compare the *cis*-influence of the central donor group. It becomes evident that the boron-based donor group in **2** exhibits the weakest *cis*-influence among this series, containing pincer-type ligands with tertiary amines[4] and phosphine-[5] as well as thioether-[6] and sulfoxide-groups.[7] This trend is con- firmed by the P–Pt-bond length, as determined by single crystal X-Ray diffraction. Within this series of cationic Pt^{II} complexes the influence of the central donor group on the Pt–Cl-bond in *trans*- position was found to be different. The shortest Pt–Cl-bond, tentatively associated with the weakest *trans*-influence is observed for the complex with a tertiary amine (2.296 Å), followed by the complex with the sulfoxide-based ligand (2.317 Å), with the thioether-based ligand (2.347 Å) and the phosphine-based ligand (2.349 Å). With a Pt–Cl-bond distance of 2.440 Å the central boron-based donor group in complex **2** exhibits by far the strongest *trans*-influence among this series.

Table S1. Spectroscopic and structural features of related cationic platinum pincer-type complexes with ancillary chorido ligands.

Complex	D =	X =	$^1J_{PtP}$ / Hz	d_{Pt-P} / Å	d_{Pt-Cl} / Å	Ref.
	BH	PPh$_2$	2991	2.291 / 2.279	2.440	
	NPh	CH$_2$	2712	2.291 / 2.300	2.296	[4]
	S	CH$_2$	2538	2.314 / 2.317	2.347	[6]
	S(O)	CH$_2$	2501	2.319	2.317	[7]
	PPh	CH$_2$	2484	2.311 / 2.315	2.349	[5]
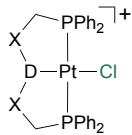
3. Spectra
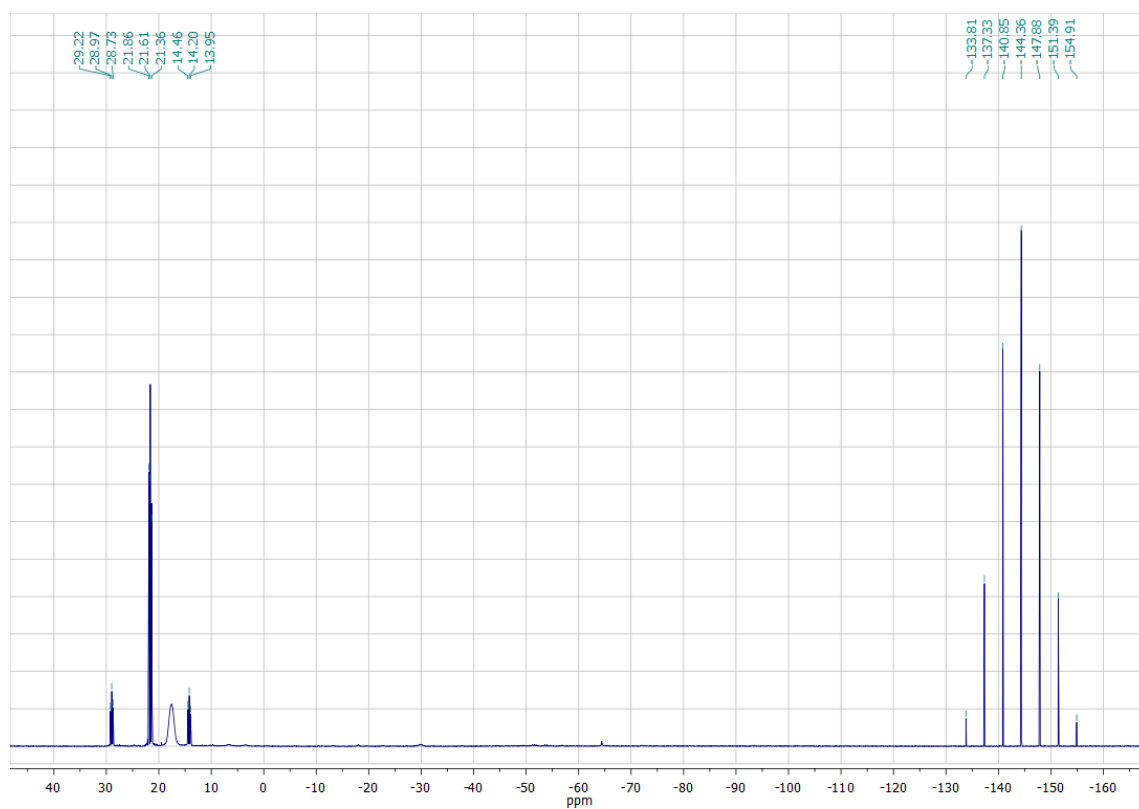
Figure 1 $^{31}P\{^1H\}$ NMR ($^{31}P\{^1H\}$ NMR (202.28 MHz, CD$_2$Cl$_2$, 27 °C) spectrum of [({dppm}$_2$BH)PtCl](PF$_6$) (**2**).
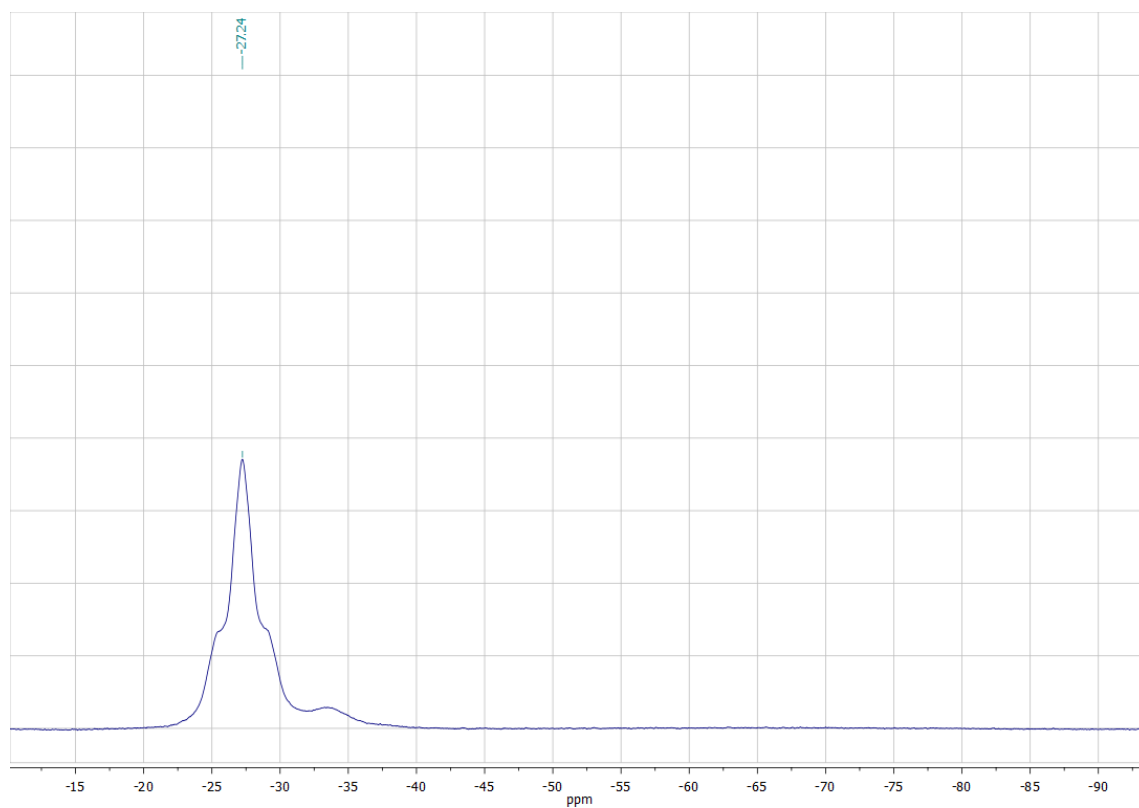
Figure 2 ^{11}B NMR (160.33 MHz, CD$_2$Cl$_2$, 27 °C) spectrum of [({dppm}$_2$BH)PtCl](PF$_6$) (**2**) .

- 8 -
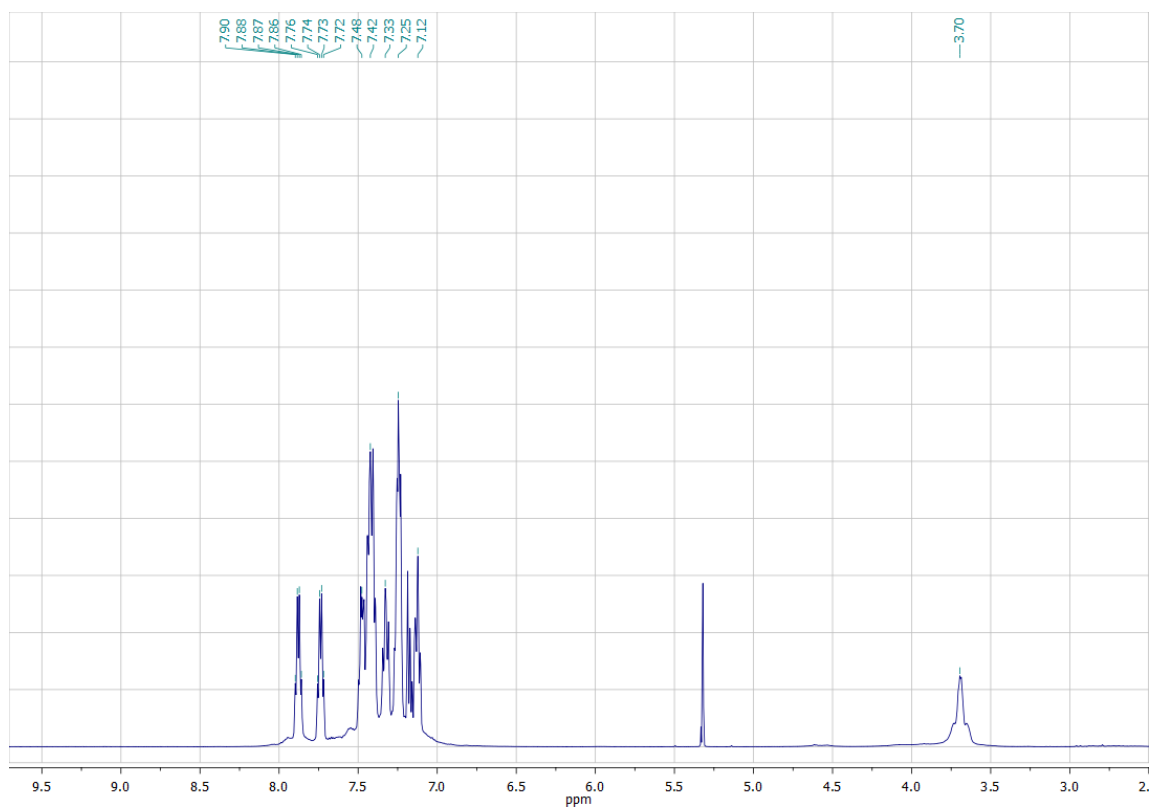
Figure 3 ^{1}H NMR spectrum (499.72 MHz, CD$_2$Cl$_2$, 27 °C) of [({dppm}$_2$BH)PtCl](PF$_6$) (**2**).
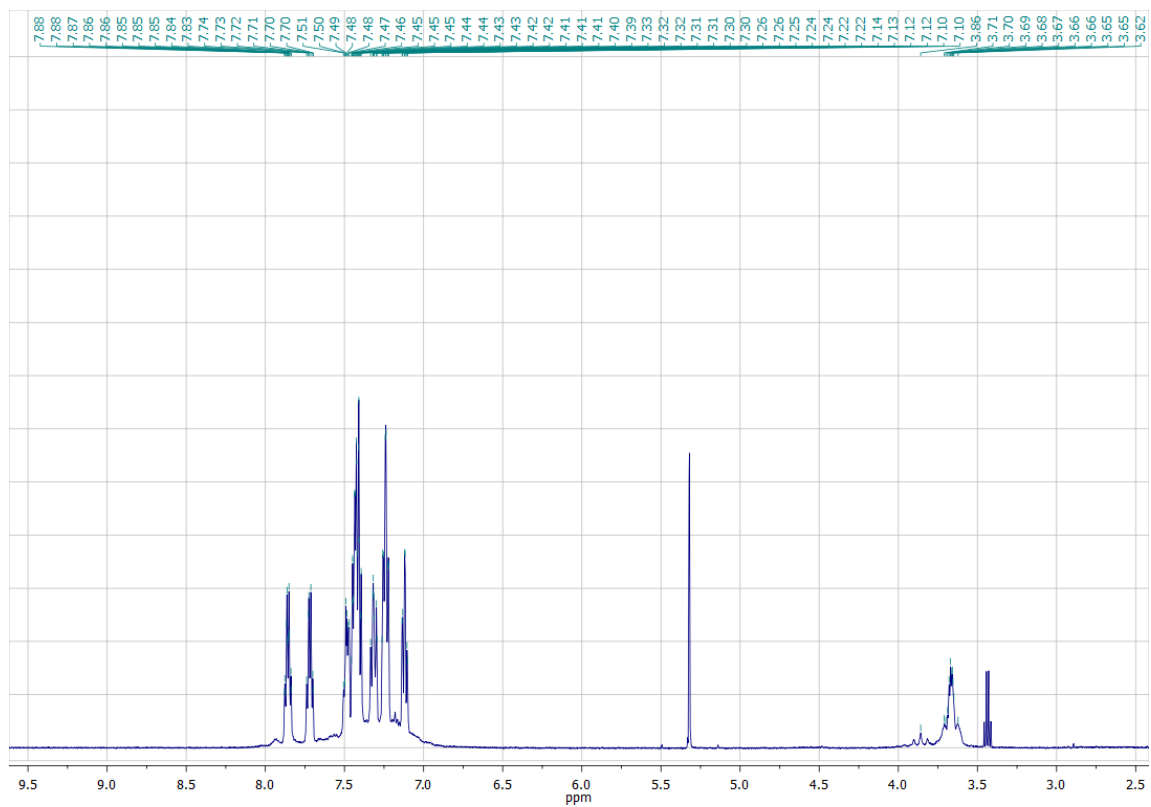
Figure 4 ^{1}H{^{11}B} NMR *(499.72 MHz, CD$_2$Cl$_2$, 27 °C)* spectrum of [({dppm}$_2$BH)PtCl](PF$_6$) (**2**).
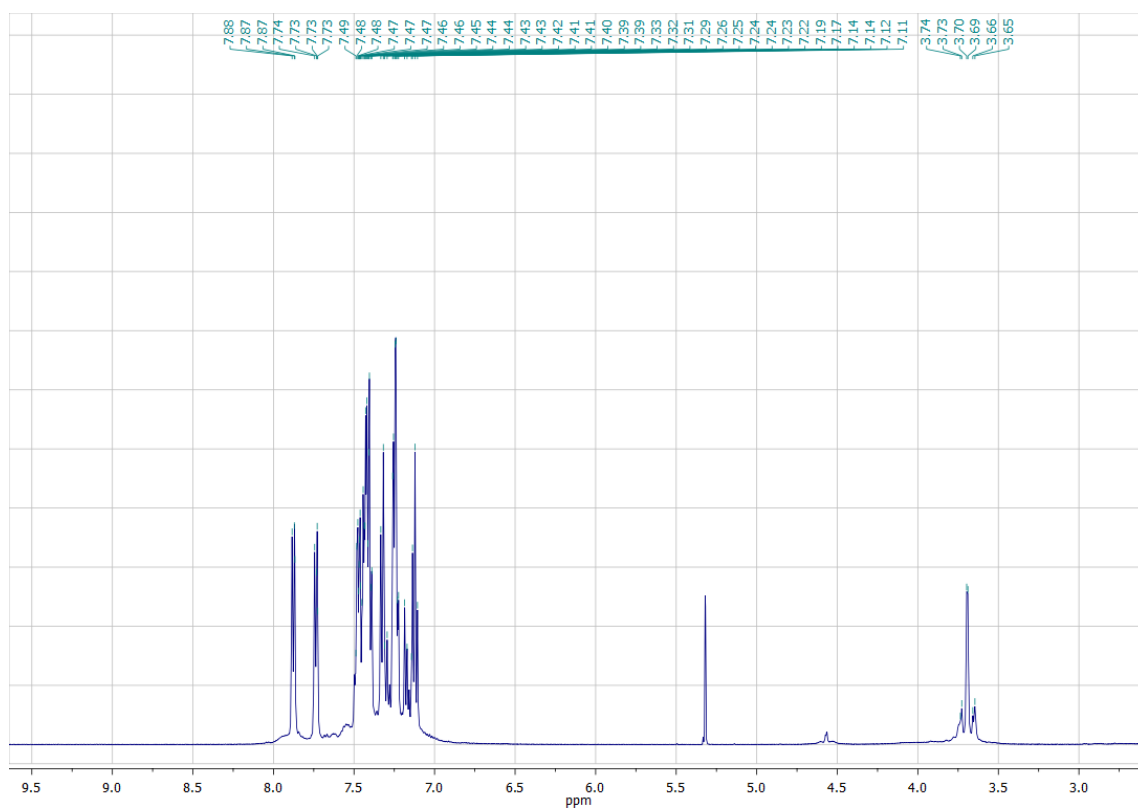
Figure 5 ^{1}H{^{31}P} NMR (499.72 MHz, CD$_2$Cl$_2$, 27 °C) spectrum of [({dppm}$_2$BH)PtCl](PF$_6$) (**2**).
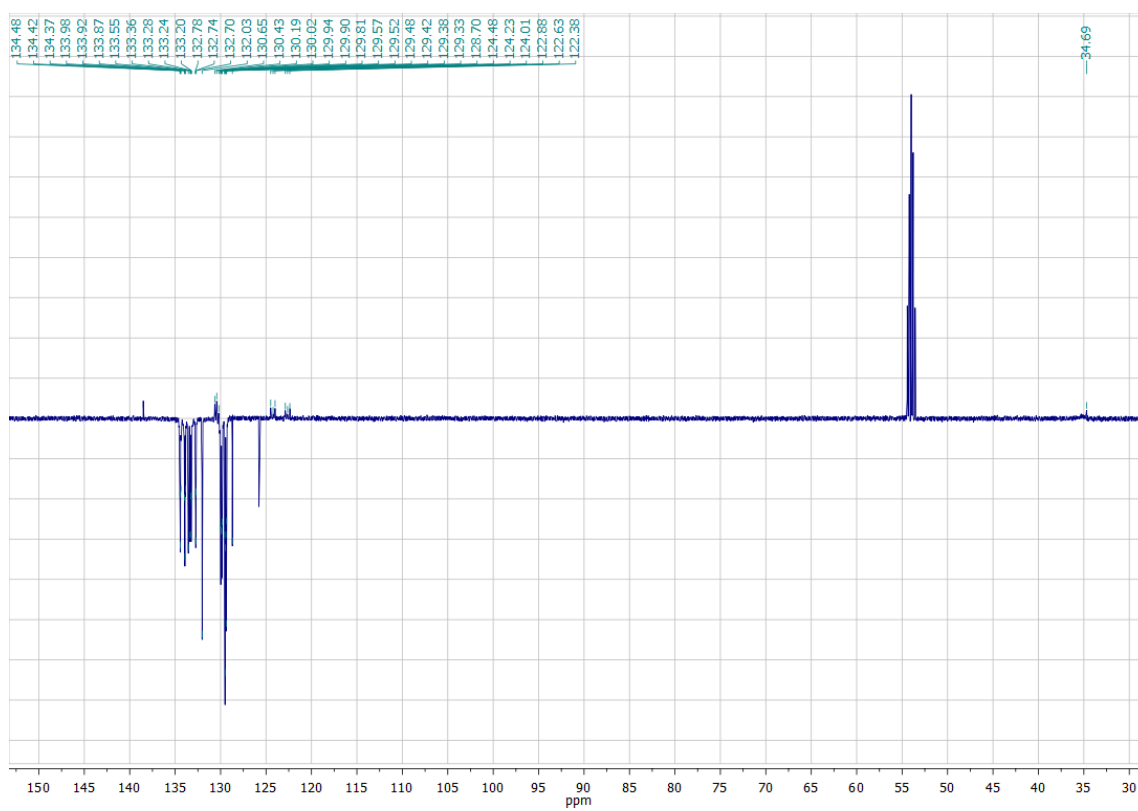
Figure 6 ^{13}C APT NMR (125.67 MHz, CD$_2$Cl$_2$, 27 °C) spectrum of [({dppm}$_2$BH)PtCl](PF$_6$) (**2**).
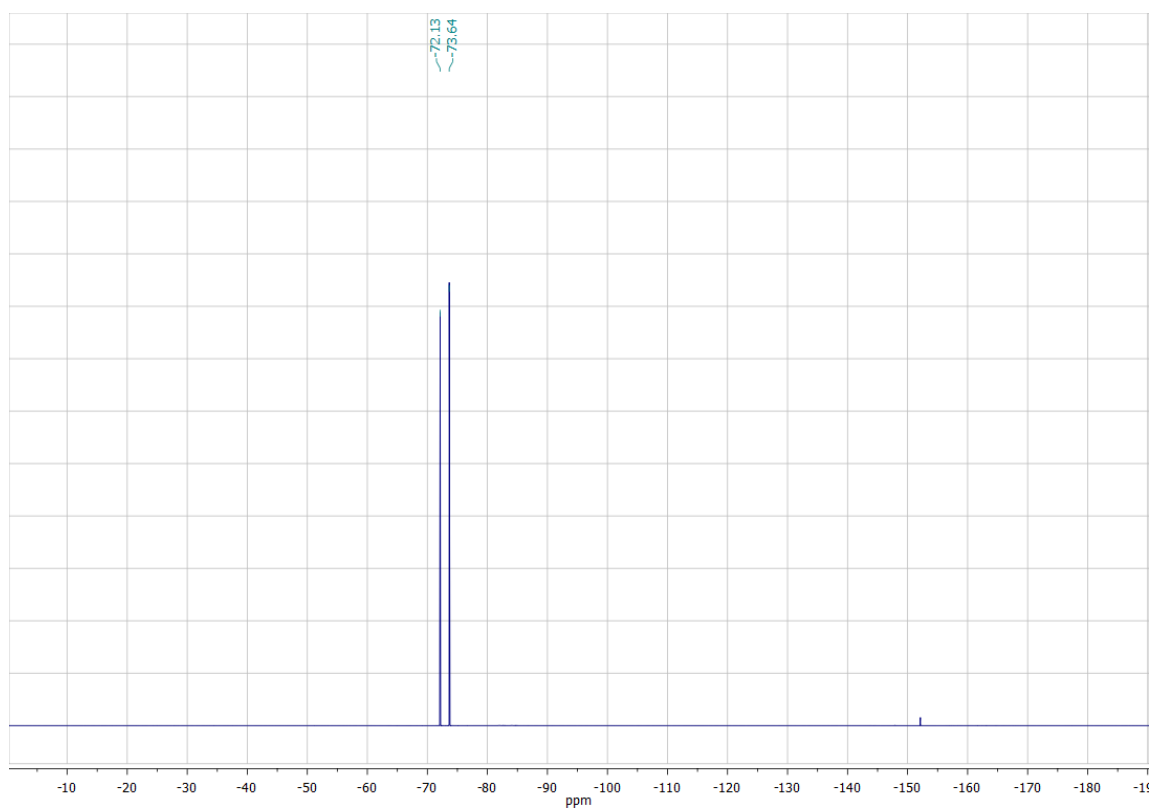
Figure 7 ^{19}F NMR (470.16 MHz, CD_2Cl_2, 27 °C) spectrum of [({dppm}$_2$BH)PtCl](PF$_6$) (**2**).
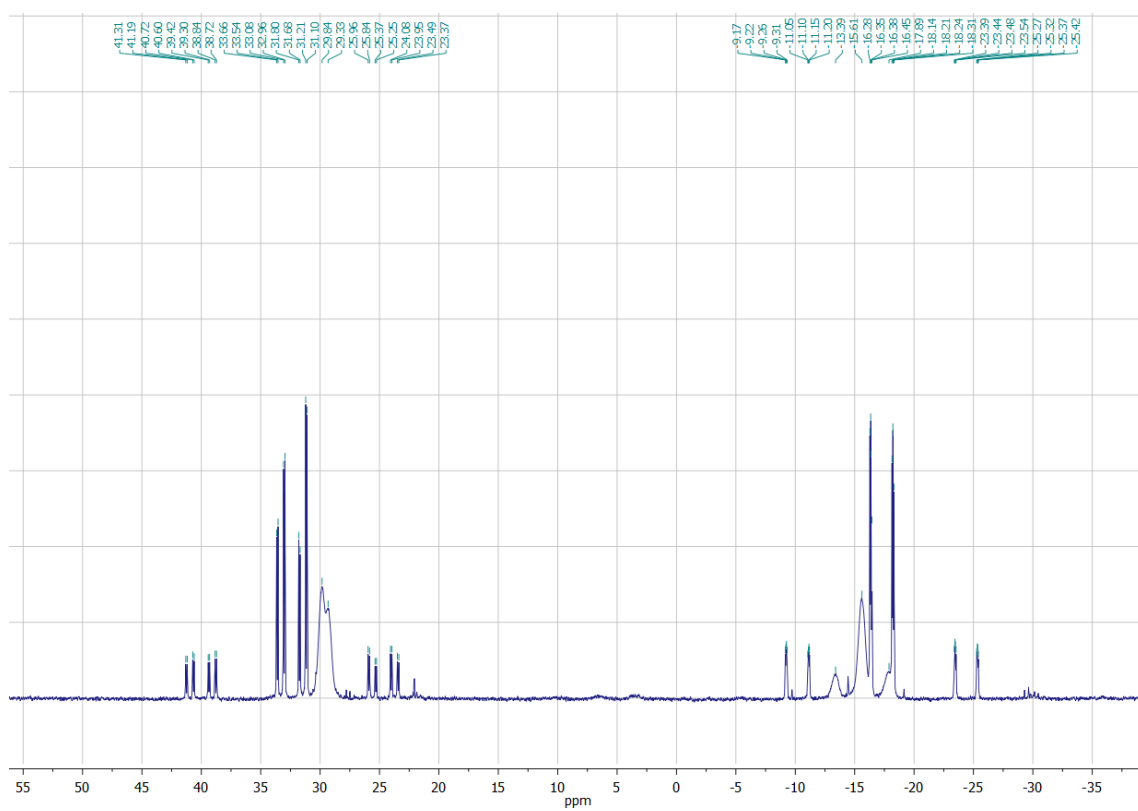
Figure 8 $^{31}P\{^1H\}$ NMR (202.28 MHz, CD_2Cl_2, 27 °C) spectrum of [(dppm)({dppm}BH$_2$)Pt](PF$_6$) (**3**).
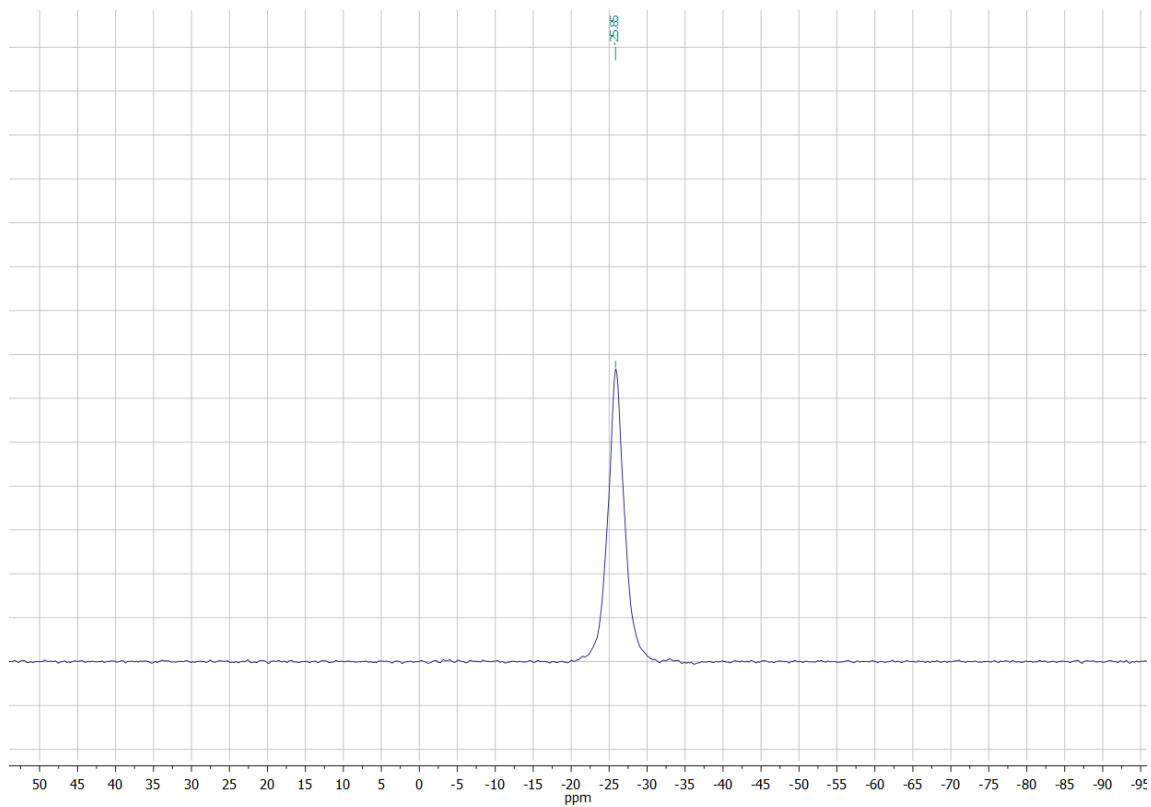
Figure 9 ^{11}B NMR (160.33 MHz, CD_2Cl_2, 27 °C) spectrum of $[(dppm)(\{dppm\}BH_2)Pt](PF_6)$ (**3**).
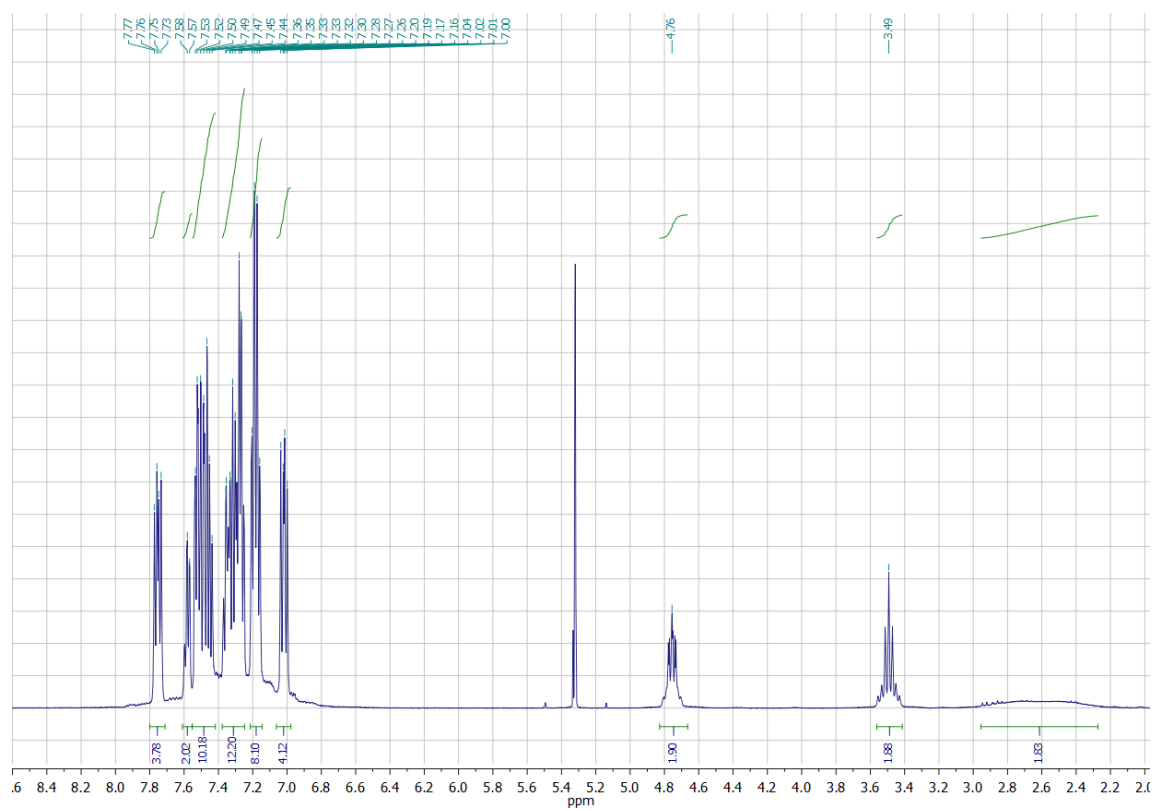
Figure 10 ^1H NMR (499.72 MHz, CD_2Cl_2, 27 °C) spectrum of $[(dppm)(\{dppm\}BH_2)Pt](PF_6)$ (**3**).
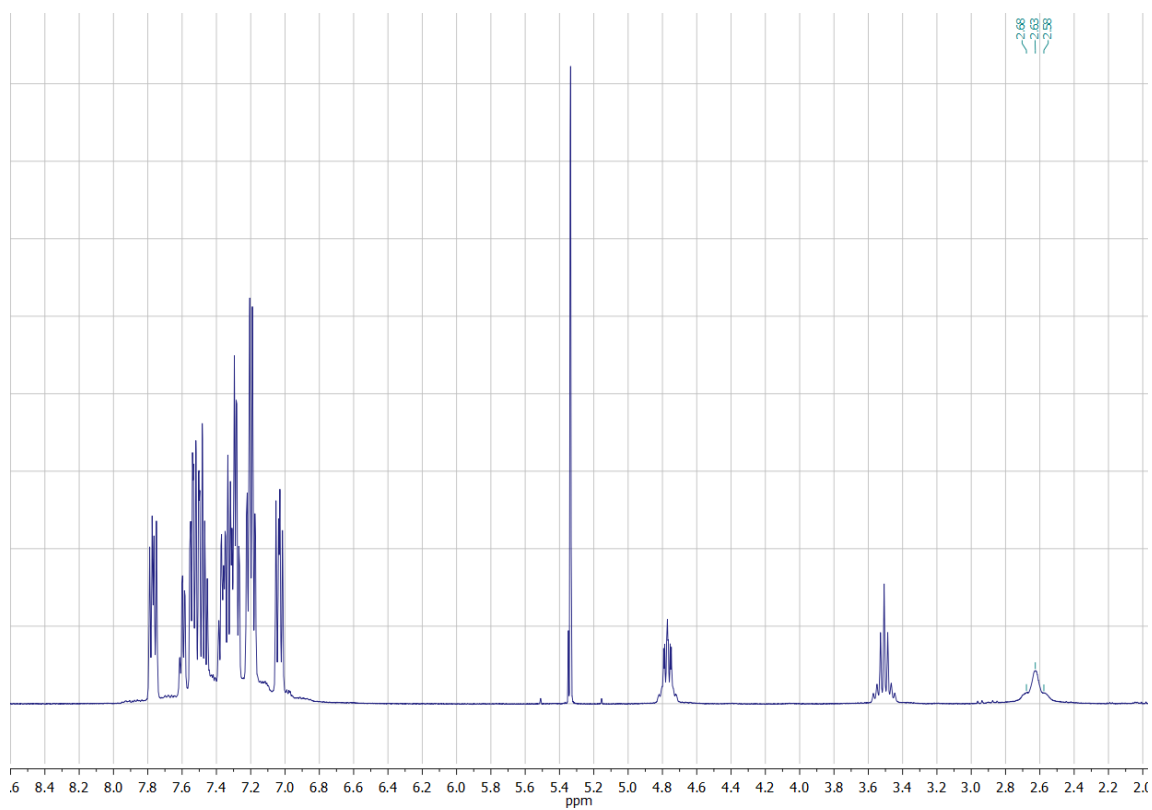
Figure 11 $^1H\{^{11}B\}$ NMR (160.33 MHz, CD_2Cl_2, 27 °C) spectrum of $[(dppm)(\{dppm\}BH_2)Pt](PF_6)$ (**3**).
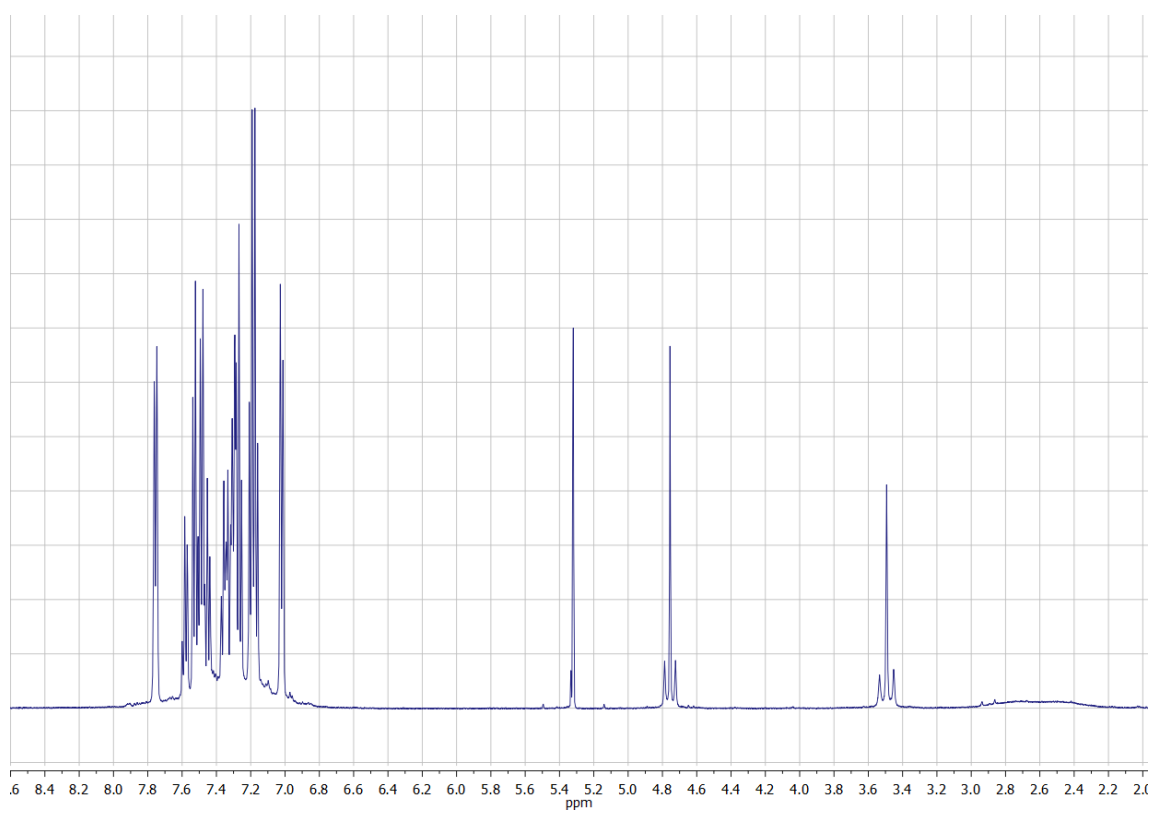
Figure 12 $^1H\{^{31}P\}$ NMR (^1H NMR (499.72 MHz, CD_2Cl_2, 27 °C) spectrum of $[(dppm)(\{dppm\}BH_2)Pt](PF_6)$ (**3**).
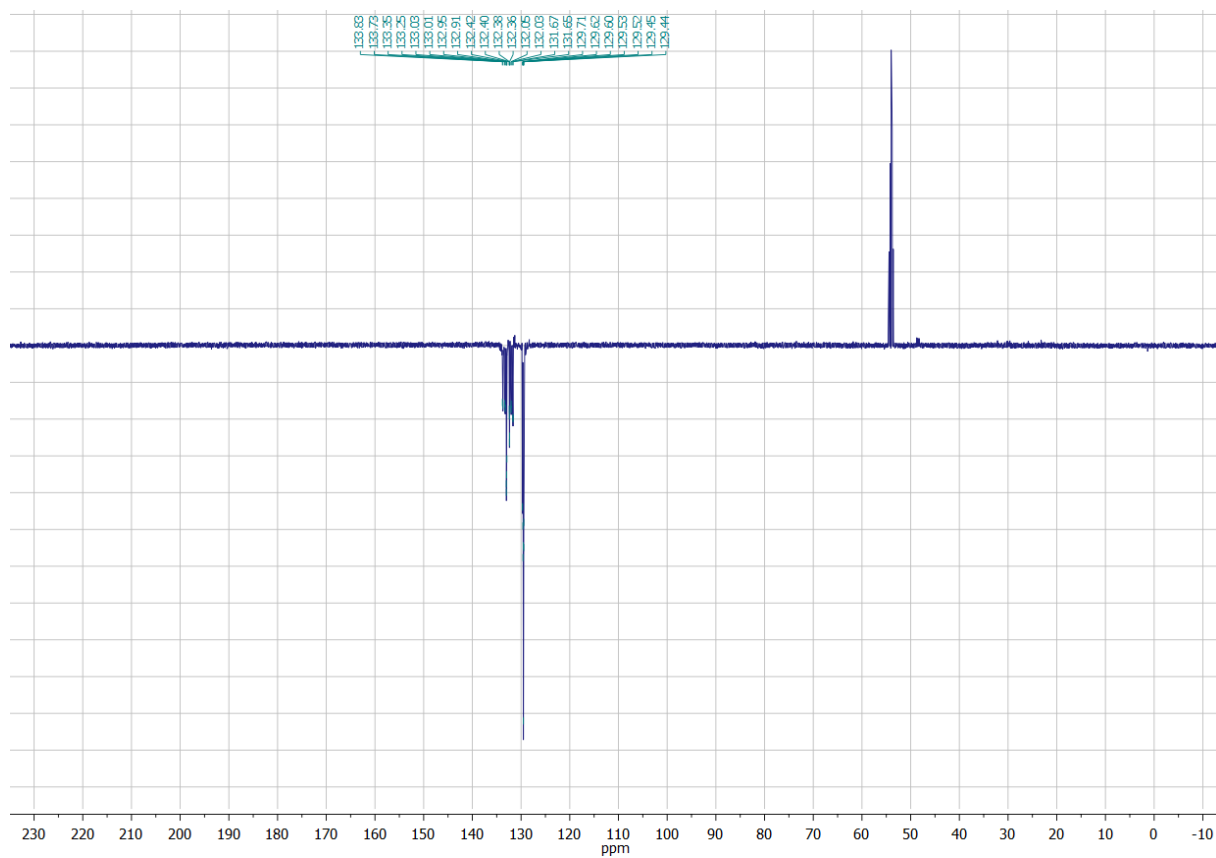
Figure 13 ^{13}C APT NMR (125.67 MHz, CD$_2$Cl$_2$, 27 °C) spectrum of [(dppm)({dppm}BH$_2$)Pt](PF$_6$) (**3**).
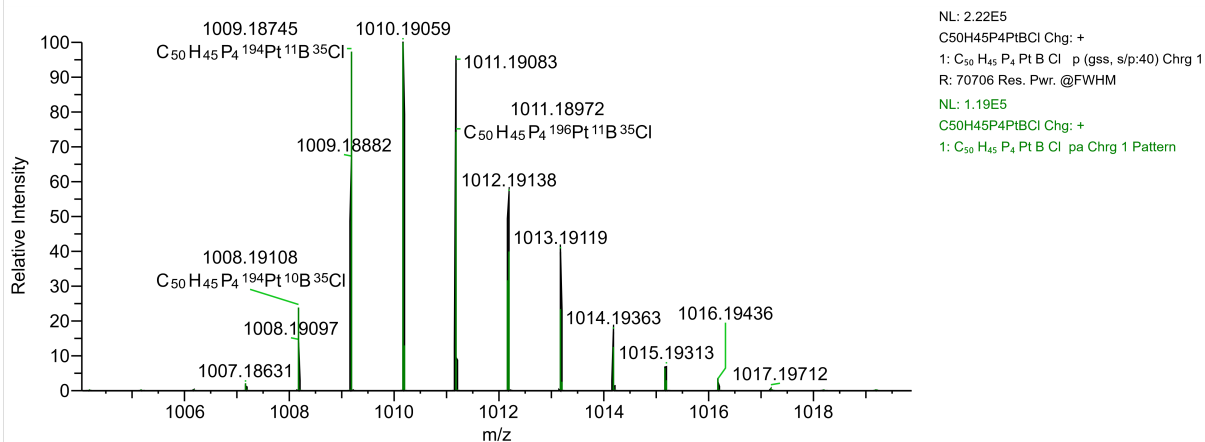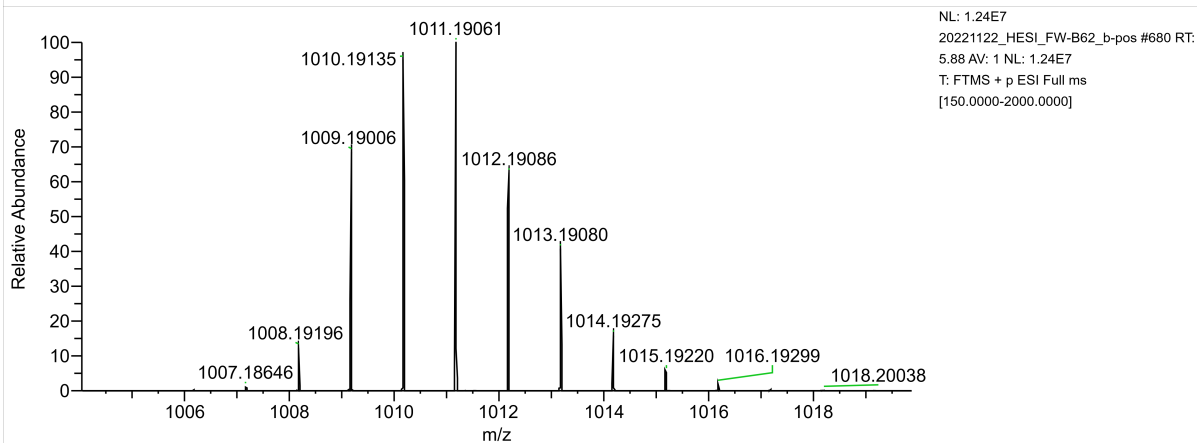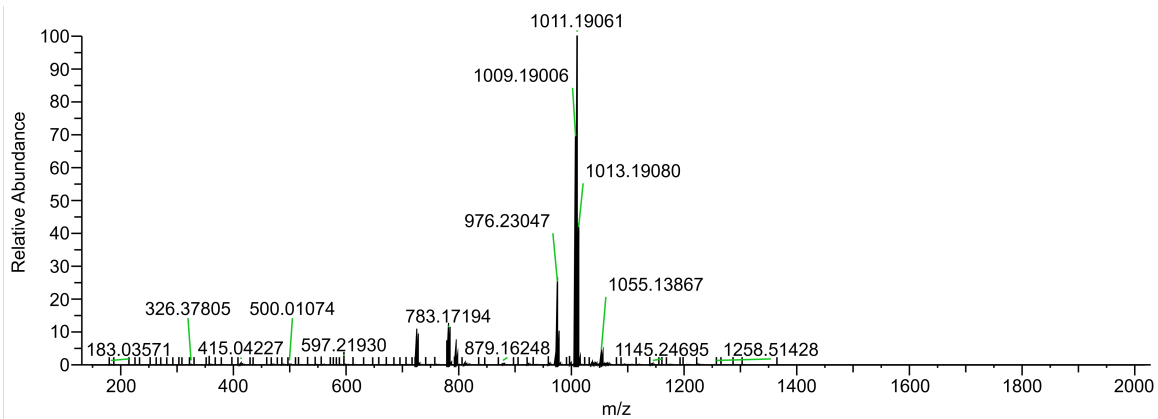
Figure 14 HR-MS spectrum (positive mode, HESI, full MS) of complex **2** (top) and of measured and calculated isotopic pattern of **2**.
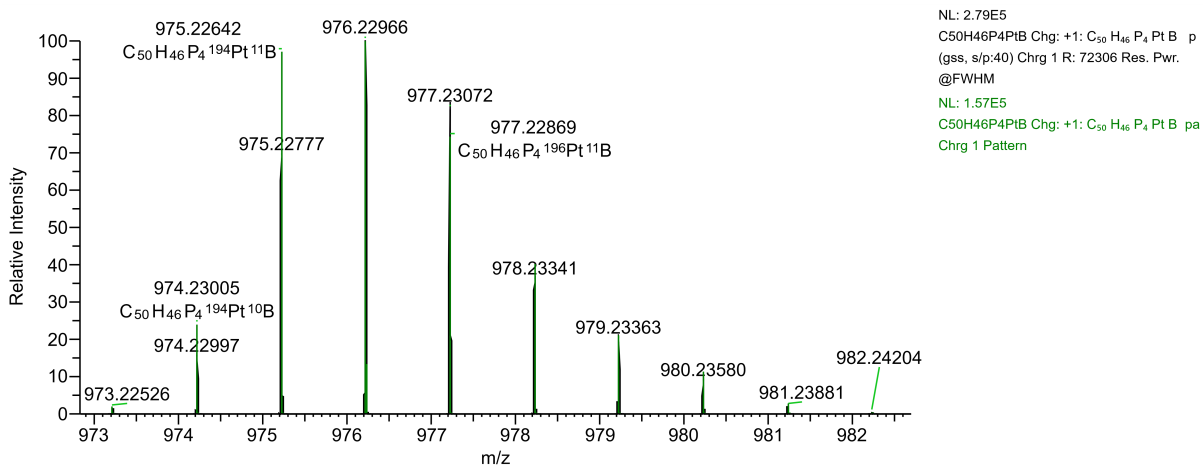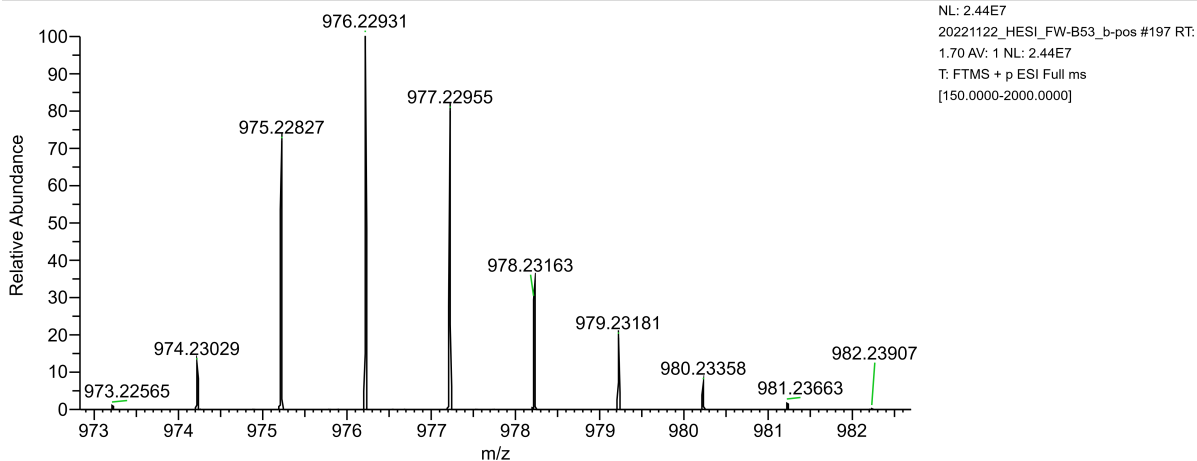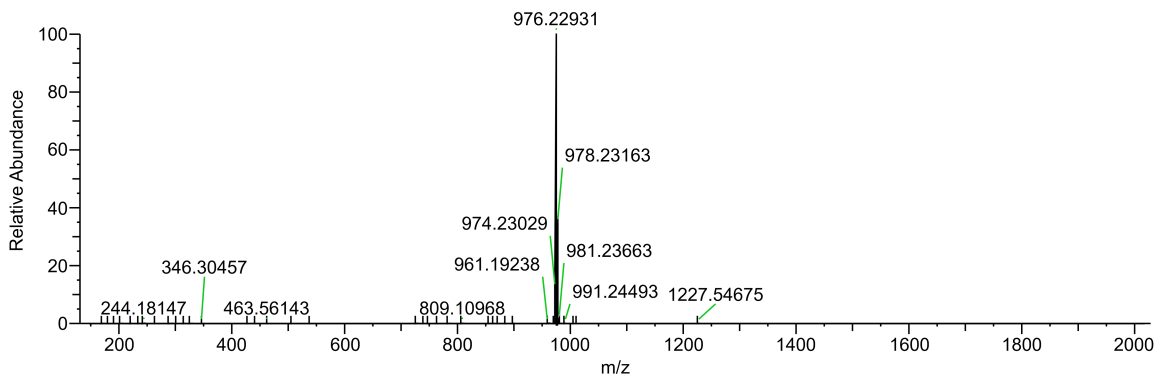
Figure 15 HR-MS spectrum (positive mode, HESI, full MS) of complex **3** (top) and of measured and calculated isotopic pattern of **3**.

4. X-Ray Crystallography

The single crystal X-ray diffraction data for the structural analysis were collected using graphite-monochromated Mo-Kα-radiation (λMoKα= 0.71073) on an imaging plate system STOE IPDS2T and IPDS2. The structures were solved with implemented SHELXT into the Olex2 software package version 1.5 by intrinsic phasing method and refined against F^2 by full-matrix-least- square techniques using SHELXL.[8–11] Crystallographic data for **2** and **3** was deposited at Cambridge Crystallographic Data Centre (CCDC 2244021 - 2244022) and can be obtained free of charge via www.ccdc.cam.ac.uk/. Selected Crystallographic data is summarized in Table S2.

Table S2. Crystallographic data of complexes **2** and **3**.

Complex	$2 \cdot Et_2O \cdot ^3/_4THF$	$3 \cdot ^1/_2toluene$
Formula	$C_{50}H_{45}BClF_6P_5Pt \cdot C_4H_{10}O \cdot ^3/_4C_4H_8O$	$C_{50}H_{46}BF_6P_5Pt \cdot ^1/_2C_7H_8$
M / g·mol^{-1}	1284.25	1167.68
T/K	170	170
Crystal System	orthorhombic	monoclinic
Space Group	$Pbcn$	$P2_1/n$
a / Å	23.859(5)	11.728(2)
b / Å	23.456(5)	26.813(5)
c / Å	20.743(4)	17.242(3)
α / °	90	90
β / °	90	102.88(3)
γ / °	90	90
V / Å^3	11609(4)	5285.5(19)
Z	8	4
$\rho_{calc.}$ / g·cm^{-3}	1.470	1.519
μ / mm^{-1}	2.660	2.862
F(000)	5168	2332
Θ_{min}/°	1.564	1.648
Θ_{max}/°	26.000	25.998
Measured Refl.	69616	44794
Independent Refl.	11412 (R_{Int} = 0.0935)	10384 (R_{Int} = 0.0946)
Ind. Refl. (I>2σ(I))	7092	8814
Parameters / Restraints	672/150	598/136
R_1	0.0510	0.0591
R_1 (all data)	0.0884	0.0693
wR_2	0.1246	0.1385
wR_2 (all data)	0.1424	0.1456
GooF	1.022	1.103
Max. peak + hole / e·Å^{-3}	1.629/-1.052	2.070 / -1.889
CCDC	2244021	2244022

Table S3. Selected bond length of complexes **2** and **3**.

Bond / Å	Complex **2**	Complex **3**
Pt–P	2.2792(17)	2.287(2)
	2.2906(17)	2.288(2)
		2.414(2)
Pt–B	2.115(7)	2.175(9)
Pt–Cl	2.4396(16)	
P–B	1.944(7)	1.913(11)
	1.949(8)	

5. Computational Details

All reported structures were optimized by the density functional theory (DFT)[12] with Grimme's B97D3 functional[13,14] and the def2svp basis set[15,16] in the gas phase using Gaussian16.[17] Frequency analysis calculations of optimized structures were performed at the same level of theory (B97D3/def2svp) to characterize the structures to be minima (no imaginary frequency) or transition states (one imaginary frequency). Based on the B97D3/def2svp optimized geometries, the energy results were further refined by calculating the single point energy at the B97D3/def2tzvp level of theory. The bulky solvation effect of CH_2Cl_2 was simulated by SMD[18] continuum solvent mode at the B97D3/def2tzvp level of theory. Intrinsic reaction coordinate (IRC) calculations were performed to confirm the connection between two correct minima for a transition state. Laplacian contour line plots (Figure 16) were created with the program Multiwfn.[14]
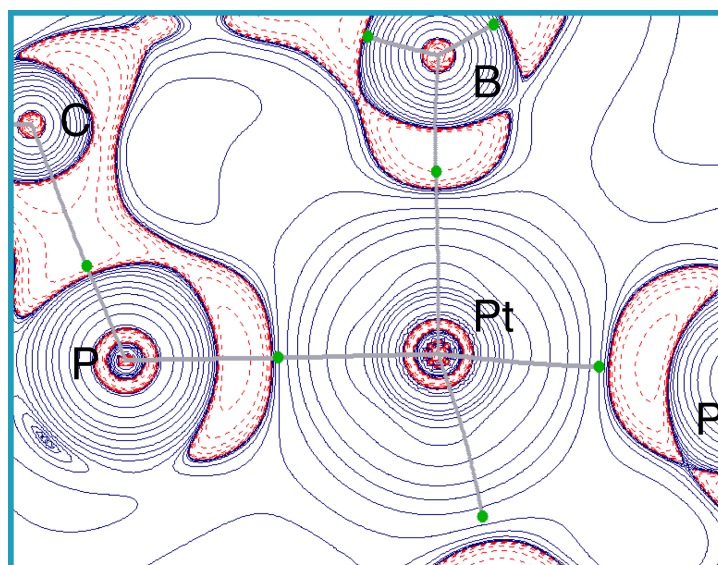
Figure 16 Contour line diagram of the Laplacian distribution $\nabla^2\rho$ in **3**. Bond critical points (3,-1) are depicted in green. Bonds are shown grey, when the distance between two atoms is lower than the sum of van der Waals radii..

 xyz-coordinates of all minima and transition states are available as separate xyz-files.

6. References

[1]   K. Sommer, *Zeitschrift für Anorg. und Allg. Chemie* **1970**, *376*, 37–43.

[2]   A. Bäcker, Y. Li, M. Fritz, M. Grätz, Z. Ke, R. Langer, *ACS Catal.* **2019**, *9*, 7300–7309.

[3]   L. Rigamonti, C. Manassero, M. Rusconi, M. Manassero, A. Pasini, *Dalt. Trans.* **2009**, *2*, 1206–1213.

[4]   S. G. Keskin, J. M. Stanley, L. A. Mitchell, B. J. Holliday, *Inorganica Chim. Acta* **2019**, *486*, 200–212.

[5]   P. Sevillano, A. Habtemariam, S. Parsons, A. Castiñeiras, M. E. García, P. J. Sadler, *J. Chem. Soc. Dalt. Trans.* **1999**, *4*, 2861–2870.

[6]   L. V. Andreasen, O. Simonsen, O. Wernberg, *Inorganica Chim. Acta* **1999**, *295*, 153–163.

[7]   S.-Y. SIAH, P.-H. LEUNG, K. F. MOK, *Polyhedron* **1994**, *13*, 3253–3255.

[8]   O. V. Dolomanov, L. J. Bourhis, R. J. Gildea, J. A. K. Howard, H. Puschmann, *J. Appl. Crystallogr.* **2009**, *42*, 339–341.

[9]   L. J. Bourhis, O. V. Dolomanov, R. J. Gildea, J. A. K. Howard, H. Puschmann, *Acta Crystallogr. Sect. A Found. Crystallogr.* **2015**, *71*, 59–75.

[10]   G. M. Sheldrick, *Acta Crystallogr. Sect. A Found. Crystallogr.* **2008**, *64*, 112–122.

[11]   G. M. Sheldrick, *Acta Crystallogr. Sect. A Found. Crystallogr.* **2015**, *71*, 3–8.

[12]   P. Hohenberg, W. Kohn, *Phys. Rev.* **1964**, *136*, B864–B871.

[13]   S. Grimme, *J. Comput. Chem.* **2006**, *27*, 1787–1799.

[14]   S. Grimme, S. Ehrlich, L. Goerigk, *J. Comput. Chem.* **2011**, *32*, 1456–1465.

[15]   F. Weigend, C. Hättig, H. Patzelt, R. Ahlrichs, S. Spencer, A. Willets, *Phys. Chem. Chem. Phys.* **2006**, *8*, 1057.

[16]   F. Weigend, R. Ahlrichs, K. A. Peterson, T. H. Dunning, R. M. Pitzer, A. Bergner, *Phys. Chem. Chem. Phys.* **2005**, *7*, 3297.

[17]   Gaussian 16, Revision C.01, M. J. Frisch, G. W. Trucks, H. B. Schlegel, G. E. Scuseria, M. A. Robb, J. R. Cheeseman, G. Scalmani, V. Barone, G. A. Petersson, H. Nakatsuji, X. Li, M. Caricato, A. V. Marenich, J. Bloino, B. G. Janesko, R. Gomperts, B. Mennucci, H. P. Hratchian, J. V. Ortiz, A. F. Izmaylov, J. L. Sonnenberg, D. Williams-Young, F. Ding, F. Lipparini, F. Egidi, J. Goings, B. Peng, A. Petrone, T. Henderson, D. Ranasinghe, V. G. Zakrzewski, J. Gao, N. Rega, G. Zheng, W. Liang, M. Hada, M. Ehara, K. Toyota, R. Fukuda, J. Hasegawa, M. Ishida,

T. Nakajima, Y. Honda, O. Kitao, H. Nakai, T. Vreven, K. Throssell, J. A. Montgomery, Jr., J. E. Peralta, F. Ogliaro, M. J. Bearpark, J. J. Heyd, E. N. Brothers, K. N. Kudin, V. N. Staroverov, T. A. Keith, R. Kobayashi, J. Normand, K. Raghavachari, A. P. Rendell, J. C. Burant, S. S. Iyengar, J. Tomasi, M. Cossi, J. M. Millam, M. Klene, C. Adamo, R. Cammi, J. W. Ochterski, R. L. Martin, K. Morokuma, O. Farkas, J. B. Foresman, and D. J. Fox, Gaussian, Inc., Wallingford CT, **2016**.

[18]   A. V. Marenich, C. J. Cramer, D. G. Truhlar, *J. Phys. Chem. B* **2009**, *113*, 6378–6396.

[19]   T. Lu, F. Chen, *J. Comput. Chem.* **2012**, *33*, 580–592.